REVIEWS

Journal of Semiconductors
(2021) 42, 031701
doi: 10.1088/1674-4926/42/3/031701

Low-dimensional materials for photovoltaic application

Rokas Kondrotas[1, 2, ‡], Chao Chen[1, ‡], XinXing Liu[1], Bo Yang[1], and Jiang Tang[1, †]

[1]Sargent Joint Research Center, Wuhan National Laboratory for Optoelectronics and School of Optical and Electronic Information, Huazhong University of Science and Technology, Wuhan 430074, China

[2]Center for Physical Sciences and Technology, Sauletekio 3, Vilnius 10257, Lithuania

Abstract: The photovoltaic (PV) market is currently dominated by silicon based solar cells. However technological diversification is essential to promote competition, which is the driving force for technological growth. Historically, the choice of PV materials has been limited to the three-dimensional (3D) compounds with a high crystal symmetry and direct band gap. However, to meet the strict demands for sustainable PV applications, material space has been expanded beyond 3D compounds. In this perspective we discuss the potential of low-dimensional materials (2D, 1D) for application in PVs. We present unique features of low-dimensional materials in context of their suitability in the solar cells. The band gap, absorption, carrier dynamics, mobility, defects, surface states and growth kinetics are discussed and compared to 3D counterparts, providing a comprehensive view of prospects of low-dimensional materials. Structural dimensionality leads to a highly anisotropic carrier transport, complex defect chemistry and peculiar growth dynamics. By providing fundamental insights into these challenges we aim to deepen the understanding of low-dimensional materials and expand the scope of their application. Finally, we discuss the current research status and development trend of solar cell devices made of low-dimensional materials.

Key words: low-dimensional materials; photovoltaic; absorption; defect; anisotropy

Citation: R Kondrotas, C Chen, X X Liu, B Yang, and J Tang, Low-dimensional materials for photovoltaic application[J]. *J. Semicond.*, 2021, 42(3), 031701. http://doi.org/10.1088/1674-4926/42/3/031701

1. Introduction

Silicon based solar cells are currently dominate with over 90% share in the photovoltaic (PV) market[1]. However, solar cell technology diversification is essential to further improve solar cell power conversion efficiency (PCE) and to increase its versatility for various applications. Multiple pn junction solar cells are believed to have the potential to become leading terrestrial PV technology exceeding 30% PCE in the future which require the development of top and/or bottom cells with high efficiency, good stability and process compatibility. With the dawning age of electrification of unmanned vehicles, planes and boats, flexible and low-cost with high power-to-weight ratio PV panels will be highly desired in these machines. Light-weight, semi-transparent solar cells with aesthetic designs, easy integration and long-term stability are required in the rapidly growing field of building integrated PV. To meet these demands, new compounds with specific physical and chemical properties have been consistently probed, and potential PV candidates are advocated.

Materials with a highly symmetrical crystal structure and direct band gap are preferred in solar cells, because it results in high absorption coefficient and isotropic carrier transport. This is especially important for polycrystalline thin films where an absorber of less than few micrometers is desirable to reduce material demand and to ensure effective carrier collection. Mainstream polycrystalline solar cell technologies such as Cu(In,Ga)Se_2, CdTe and $CH_3NH_3PbI_3$ all have a highly symmetrical crystal structure and have demonstrated over 22% PCE[2]. However, elemental abundance, environmental restrictions, thermodynamic stability and necessity for a broader range of band gaps (E_g) have fueled the exploration of new PV candidates[3]. To meet these demands, material space has been expanded by increasing the number of components in the compound, such as from unary (Si) to quaternary (pentanary) $Cu_2ZnSn(S,Se)_4$, while retaining high crystal symmetry. Nonetheless, the complexity of the material increases progressively with each addition of atom(s) in the primitive cell, which impedes the control of phase purity, point defects, formation of secondary phases and consequently solar cell performance[4].

There is a group of compounds with binary and ternary compositions as well as PV-relevant characteristics, which have not been studied extensively because of their reduced structural dimensionality. Low-dimensional materials (namely layered (2D) and chained (1D), see Fig. 1) might be considered to be unsuitable for PV application but have been shown to have potential, both theoretically and experimentally[5–7]. The calculated spectroscopic limited maximum efficiency (SLME) for an absorber thickness of only 200 nm for two-dimensional (2D) $CuSbSe_2$ and one-dimensional (1D) Sb_2Se_3 was 27% and 28%, respectively, in contrast to 3D $CuInSe_2$ (23%), 3D Cu_2ZnSnS_4 (22%) and 3D CdTe (20%)[8, 9]. A remarkable 9.2% PCE has recently been reported for 1D Sb_2Se_3-based solar cells[10], ranking as the second highest Earth-abundant non-toxic thin film solar cell technology within only 7 years of dedicated research. Successful application of low-dimensional materials has not only been limited to PV, but they have also been used in photocatalysis[11], ultra-high mobility transistors[12, 13], thermoelectrics[14], piezoelectrics[15], optics[16] and so on.

Rokas Kondrotas and Chao Chen contributed equally.
Correspondence to: J Tang, jtang@mail.hust.edu.cn
Received 4 AUGUST 2020; Revised 27 SEPTEMBER 2020.

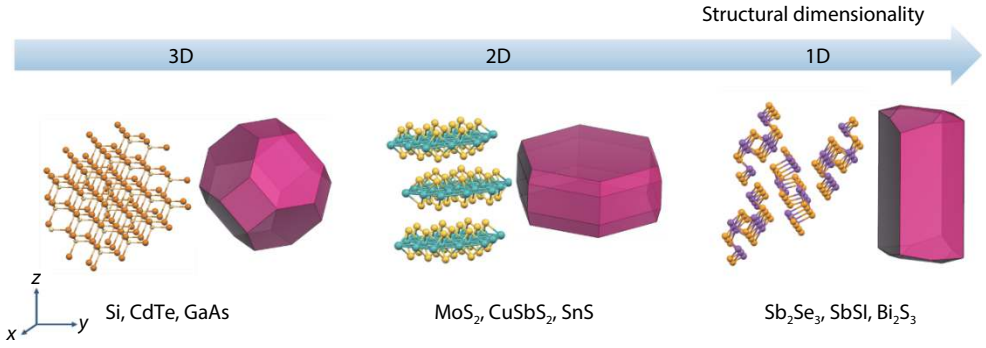

Fig. 1. (Color online) The evolution of crystal structure and morphology of the grain as a function of structural dimensionality. CdTe, MoS_2 and Sb_2Se_3 structures were selected as representative materials in each case. Grain morphology was calculated using Bravais–Friedel–Donnay–Harker (BFDH) theory[18].

Table 1. Summary of low-dimensional material characteristics and champion solar cell PCE.

Material	Dimension	E_g^{ind} (eV)	ΔE_g (eV)	Anisotropy ratio*	PV solar cell PCE (%)	Application
$(BA)_2(MA)_{n-1}$ Pb_nI_{3n+1}	2D	1.5–2.3	0	0.28μ[34]	12.53[35]	LED, PV solar cells
SnS	2D	1.07	0.15	0.08μ[36]	4.36[37]	Thermoelectrics, PV solar cells
SnSe	2D	0.86	0.2	0.2σ[38]	N/A	Thermoelectrics
$CuSbSe_2$	2D	1.04	0.04	N/A	4.7[39]	PV solar cells, thermoelectrics
$CuSbS_2$	2D	1.4	0.05	0.15m*[40]	3.22[41]	PV solar cells, thermoelectrics
$MoSe_2$	2D	1.06	0.40	~0.001–0.01σ[42]	1.29[43]	PEC, HER, batteries, transistors, PV solar cells
MoS_2	2D	1.29	0.30	0.006σ[44]	2.8[45]	PEC, HER, batteries, transistors, PV solar cells
GeSe	2D	1.1	0.10	0.33σ[46]	1.48[47]	PV solar cells
Sb_2Se_3	1D	1.05	0.13	~0.10σ[48]	9.2[10]	PV solar cells
Sb_2S_3	1D	1.7	0.08	~0.10σ[49]	7.5 [50]	PV solar cells, HTL
$Sb_2(S,Se)_3$	1D	1.49	N/A	N/A	10.5[51]	PV solar cells
Bi_3S_3	1D	1.35	0.10	0.32μ[52]	0.75[53]	Thermoelectrics, PV solar cells
SbSI	1D	2.15	0.20	0.31σ[54]	3.05[55]	PV solar cells, ferroelectric
BiOI	2D	1.93	0.4	N/A	1.82[56]	PV solar cells
Se	1D	1.84	0	N/A	~6.5[57]	PV solar cells

Anisotropy ratio expressed in terms of: μ - mobility, m - effective mass, σ - conductivity.

There are some excellent reviews on low-dimensional nanomaterials for catalysis, electronics and photonic applications[17]. However, we take a different angle on low-dimensional materials analyzing their unique properties in their bulk form, with a special focus on PV application. The fundamentals in particular electronic bands, surface states, defects and growth kinetics are discussed, emphasizing the contrast with 3D compounds, and paving the path for optimization of future technologies that are based low-dimensional materials.

Throughout this review we probe material properties that are critical for PV application and correlate them with unique features of low-dimensional materials. In principal, the key condition for good PV material is that diffusion length of photo-generated carriers should be larger than the light penetration depth and can be expressed as $1/\alpha < \sqrt{\mu\tau kT/q}$, where α, μ, τ, T, k and q corresponds to absorption coefficient, carrier mobility, carrier lifetime, temperature, Boltzmann constant and elementary charge, respectively. Evidently, a trade-off of α, μ and τ, to some extent, are interconnected will essentially define suitability of material for PV.

2. Low-dimensional materials for photovoltaic application

2.1. Absorption and band gap

Direct band gap semiconductors are highly favored in many optoelectronic devices and would also be the first prerequisite for an absorber in solar cells. However, providing the difference between direct and indirect gaps, ΔE, is small, semiconductor can be characterized as quasi-indirect type, showing both direct- and indirect-like properties. These characteristics are quite common in low-dimensional materials (Table 1) and, as we will show, are highly suitable for PV devices.

Indirect transition requires the participation of phonon(s) which leads to a lower absorption event probability and therefore low absorption coefficient. However, when the energy of photons is equal or greater than direct gap (Fig. 2(a)), absorption increases abruptly. Therefore, assuming that the ratio of proportional constants between direct and indirect absorption is one tenth, we have calculated the number of photons absorbed in indirect semiconductor with a thickness of 2 μm as a function of ΔE using AM1.5G solar spectrum (dashed line-I in Fig. 2(b), Fig. S1 and Fig. S2). If the indirect band gap of absorber is lower than 1.35 eV, then 85% of photons will be absorbed when ΔE is in the range of 0.125–0.175 eV. For larger band gap absorbers (> 1.35 eV), the conditions are stricter requiring ΔE to be lower than 0.125 eV because of lower photon flux density in the shorter wavelength region of solar spectrum. Evidently, on a theoretical basis, a large part of the solar radiation can still be absorbed by an indir-

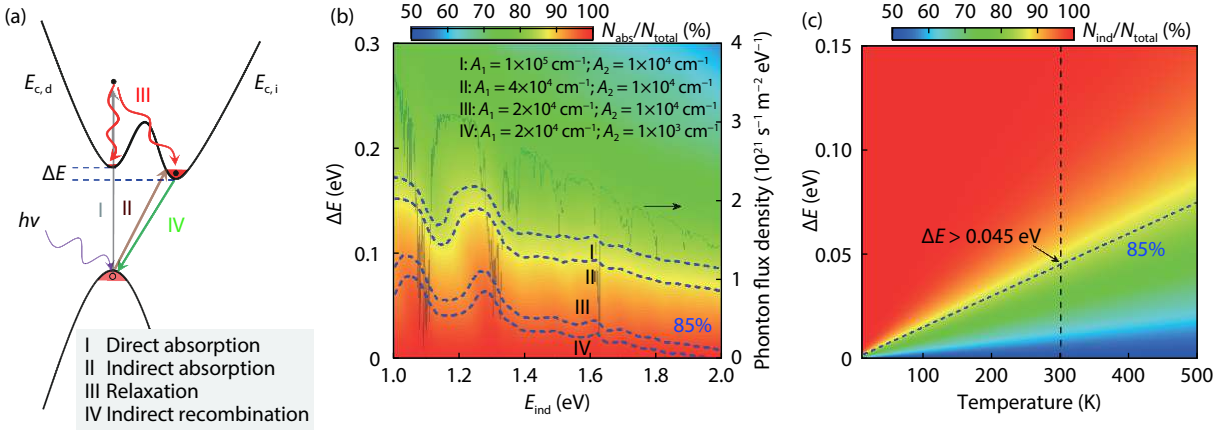

Fig. 2. (Color online) (a) Photon absorption and carrier dynamics for a quasi-indirect band gap semiconductor. Photons are first absorbed via direct band gap (I) or indirect band gap (II), they then thermodynamically relax to the indirect band gap (III) and eventually recombine (IV). (b) The ratio of photons absorbed to the total number of photons (N_{total}, photon number in AM 1.5 G spectrum with energy larger than E_{ind}) as a function of ΔE and E_{ind}. The blue-dashed line indicates a boundary of the 85%. A_1 and A_2 of dashed line 1 are 10^5 and 10^4 cm^{-1}; A_1 and A_2 of dashed line 2 are 4×10^4 and 10^4 cm^{-1}; A_1 and A_2 of dashed line 3 are 2×10^4 and 10^4 cm^{-1}; A_1 and A_2 of dashed line 4 are 2×10^4 and 10^3 cm^{-1}. (c) The ratio of electrons in indirect band (N_{ind}) to the total number of electrons (N_{total}) as a function of ΔE and temperature.

ect band gap semiconductor providing that ΔE does not exceed 0.175 eV. Although we have used typical values of absorption parameters (A_1 and A_2, defined as the proportional constants between absorption coefficient and $(h\nu - E_g)^{1/2}$ and $(h\nu - E_g)^2$, respectively), requirement for ΔE can range (decrease or increase) depending on the material's absorption capabilities. For instance, for materials with low absorption, ΔE is required to be below 0.1 eV to absorb the same number of photons (Fig. 2(b), dashed line-III, IV).

2.2. Carrier recombination and lifetime

Besides the light absorption, another key parameter to evaluate the potential of PV material is the carrier lifetime. There is a general consensus that an absorber with > 1 ns of carrier lifetime is necessary to achieve PCE of solar cell over 10%[19]. In the indirect band gap materials, because of the same momentum conservation requirement radiative carrier lifetime, τ_{rad}, is generally longer than in direct gap materials. When electrons are excited into the conduction band by absorption of the photons, carrier redistribution (intervalley scattering) occurs within hundreds of femtoseconds[20], which is faster than recombination. Under these quasi-equilibrium conditions electrons will obey Fermi-Dirac distribution and occupy the bottom of direct and indirect conduction bands proportionally. Based on Fermi-Dirac statistics we have calculated that 85% of all excited electrons will distribute in the indirect conduction valley when ΔE is larger than 0.045 eV at room temperature (Fig. 2(c) and Supplementary). Consequently, 85% of electrons will recombine via slow indirect recombination pathway resulting in the longer τ_{rad}. Commonly, defect-assisted (Shockley-Read-Hall) recombination limits the carriers' lifetime rather than radiative. Even then, simulation shows that the effective carrier lifetime, expressed as $1/\tau_{eff} = 1/\tau_{rad} + 1/\tau_{SRH}$, in an indirect band gap semiconductor will be longer than in direct assuming that electrically active trap density does not exceed 3×10^{14} cm^{-3} (Fig. S2).

When ΔE is in the 0.045–0.175 eV range (for highly absorbing materials) semiconductor can be described as quasi-indirect gap type because of direct-like absorption and indirect-like recombination characteristics. These features are highly desirable in PV materials because they lead to a sufficiently high absorption and long carrier lifetime without sacrificing one or the other. Recently, the quasi-indirect character has been observed in methylammonium lead iodide ($CH_3NH_3PbI_3$) perovskite (ΔE = 0.04–0.07 eV)[21], which has been considered to originate from spin–orbit-coupling-related Rashba splitting or collective orientations of the organic cations. Therefore, $CH_3NH_3PbI_3$ perovskite demonstrate strong optical absorption and long carrier lifetime, thus being an excellent material for solar cell application[22].

We acknowledge that quasi-indirect band gap is not a unique feature of low-dimensional materials, but due to low crystal symmetry they possess an indirect type band gap (Table 1). Therefore, materials with low-symmetry structure offer many ways to fully exploit quasi-indirect characteristics, which is highly desirable in PV applications.

2.3. Defects and doping

Understanding the formation of defects and impurities in the semiconductors allows the control of its electrical properties and is important for optimization of functional optoelectronic devices[23]. The concentration of deep "killer" defects defines carrier lifetime which is one of the critical parameters described above, whereas shallow defects are used to tune semiconductor's conductivity and its conduction type. In principle there are two generic approaches to introduce doping: (i) intrinsic, when growth conditions are adjusted to favor the formation of native point defects with low ionization energy; and (ii) extrinsic, when impurity atoms (with higher (lower) number of valence electrons) are introduced into the lattice intentionally. Both strategies are commonly implemented in semiconductors, extrinsic being more prevalent in Si, Ge, III–V and II–VI family materials and intrinsic in $Cu(In,Ga)Se_2$, $Cu_2ZnSnSe_4$ and CdTe. The formation of defects (extrinsic or intrinsic) is always followed by structural changes in the crystal lattice. In 3D materials, large structural distortion results in high formation enthalpy of particular defect. However, in low-dimensional materials, due to exist-

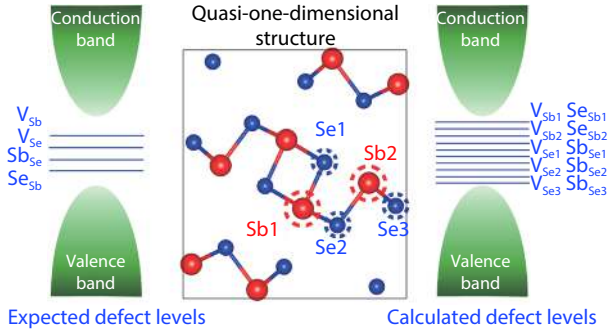

Fig. 3. (Color online) Point defects in Sb_2Se_3 taking into account, it contains two kinds of Sb and three kinds of Se. Reprinted from Chen *et al.*[27] with permission.

ence of voids (gaps) between layers or ribbons, structural deformation can be accommodated without significant energy penalty. This leads to some of the abnormal defect chemistry seen in the low-dimensional materials, including low formation energy of substitutional cation on anion and interstitial type defects[24, 25], and unusual acceptor character of anion on cation type defects[26, 27]. Additionally, in some low-dimensional materials due to asymmetric coordination environment, the same atom can occupy several (or more) inequivalent lattice sites and lead to distinctive defect properties resulting in the complex defect chemistry even for simple binary composition compounds (Fig. 3). To apprehend the defect properties in the material, first principal calculations provide best tools. However, we note that the landscape of low-dimensional materials defect chemistry will be more complicated because of their low crystal symmetry and higher structural distortion tolerance.

2.4. Anisotropy and mobility

Low structural dimensionality leads to the restricted electronic dimensionality and therefore to highly anisotropic carrier movement[28]. The degree of anisotropy (e.g. in terms of conductivity) depends on the low-dimensional material and can vary from 0.001 (for $MoSe_2$) to 0.33 (GeSe), as detailed in Table 1. This will inevitably affect photo-generated carrier transport across the absorber and consequently performance in the PV device (Fig. 4(a)). Zhou *et al.* found that the PCE of 1D Sb_2Se_3 solar cells can be almost doubled when absorbers are oriented with *c*-axis (covalently bonded) inclined rather than parallel to the substrate[29]. In addition, van der Waals (vdW) surfaces having no dangling bonds do not introduce surface states which could potentially act as recombination centers or carrier traps (Fig. 4(b)). It was shown that (*hk*0) surfaces in 1D Sb_2Se_3 have clean bandgaps, i.e. no energy states within the gap[29]. The orientation of the absorber results in either electrically benign grain boundaries or low-density defects at interfaces, in analogy to the van der vdW heterojunction. Additionally, in low-dimensional materials, vdW heterojunctions can be potentially realized which offer high quality and sharp interfaces[30]. Interfaces with low recombination velocity provide possibilities to reduce absorber thickness, and therefore mitigate the requirements for high quality (low bulk defect density) absorbers. The importance of crystallographic orientation for 2D $CuSbS_2$ absorbers for device performance was also stressed by Welch *et al.*[31].

Mobility is one of the parameters describing the transport of photo-generated carriers is the mobility. Assuming zero-optical phonon scattering model carrier mobility depends on effective mass because $\mu - m^{*-5/2}$[32]. m^* is direction dependent and typically large along the direction perpendicular to vdW planes, and therefore will result in relatively low mobility even in single crystals[33]. Therefore, to maximize carrier collection efficiency in solar cells with low-dimensional absorbers, the control of orientation will be of paramount importance.

2.5. Surface properties

Another aspect of low-dimensional materials is the large difference in the surface energies of specific facets. This originates from the fact that surfaces terminated by vdW bonds will not produce dangling bonds and will result in low surface energy[58]. For instance, calculated surface energy of 2D $CuSbSe_2$ vdW plane (001) was 0.18 J/m^2, which is two-fold lower than the second lowest surface energy of (201) facet, leading to a strong preferred (001) texture in polycrystalline films[59]. In Si and Ge, for instance, the difference between two lowest surface energies is only ~20%[60]. Although there is no direct correlation between surface energy and electron ionization potential (IP) or electron affinity (EA), planes with large difference in surface energy will inevitably have distinct IP and EA[61]; see Fig. 5. Such a case encountered in polycrystalline absorbers can lead to a non-optimal band alignment although with the same buffer layer and therefore pinned open circuit voltage and consequently solar cell performance. Welch *et al.* calculated that (001) and (010) surfaces of 2D $CuSbS_2$ can have conduction band offset difference of 0.55 eV with the same buffer layer leading to a reduced open-circuit voltage as a result of cliff-like band alignment[31]. Exemplary cases of SnS and $CuSbS_2$ strongly suggest that other low-dimensional materials will also suffer from a large difference in IP and EA of covalent (vdW) terminated surfaces.

2.6. Growth kinetics

The growth principals of low-dimensional materials will differ from 3D because of severe bonding anisotropy. For instance, the classical island growth regime in 3D crystals occurs when atoms are bonded stronger with each other than with substrate, leading to an island-like morphology (Fig. 6(a)). In the case of low-dimensional materials under the same growth conditions, atoms will prefer to bond with each other. However because of large difference in bond strength, adatoms will be preferably attached along the strong bond axis (Fig. 6(b), red arrow). This will lead to the growth of nanowires or sheets parallel to the substrate, which is more characteristic to the layer-by-layer growth regime than the island regime. In 3D materials, a strong interaction of adatoms and substrate atoms will result in layer-by-layer growth regime because the most energetically favored position will be at the terrace forming strong bond with substrate and growing layer (Fig. 6(c)). For low-dimensional materials, a strong interaction with the substrate will lead to nuclei orientation perpendicular to the surface (in terms of strong bond direction), and therefore positions on top of growing nuclei and on substrate will be equally favored leading to growth of nanowires or sheets normal to the substrate (akin to the island-like growth regime), Fig. 6(d). This hypothetical model shows the

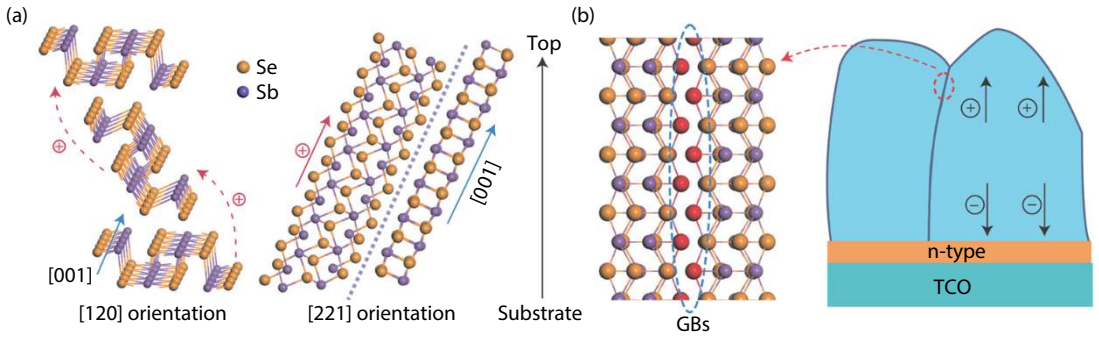

Fig. 4. (Color online) (a) Carrier movement in Sb_2Se_3 along [120] (red dashed arrows) and [221] (solid red arrow) directions. (b) Atomistic view of Sb_2Se_3 grain boundary oriented [001] direction perpendicular to substrate. All of the atoms at the edge of these ribbons are saturated (highlighted as red spheres) and introduce no recombination loss at the GBs. Reprinted from Tang *et al.* with permission[29].

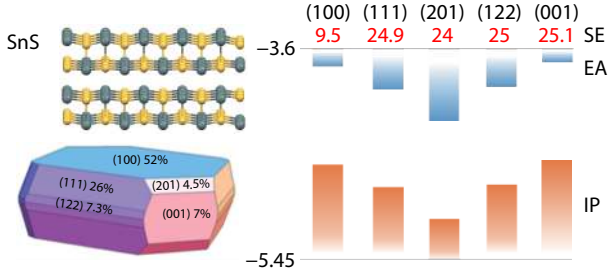

Fig. 5. (Color online) Layered crystal structure of SnS with Pnma space group and calculated morphology of the grain based on the surface energy. Surface energy (SE), EA and IP of various SnS facets. Printed with permission[61].

fundamental difference in growth dynamics of 3D and low-dimensional materials and highlights the importance of the substrate to control film orientation.

In thin film solar cells, polycrystalline substrates are commonly employed and therefore will lead to the growth of films with more dispersed orientations than presented above. Commonly, on polycrystalline substrates, the orientation of 3D materials adopts close-packed plane parallel to the surface, i.e. (111) for cubic, (112) for tetragonal or (0001) for hexagonal crystal structures. In contrast, for low-dimensional materials the substrate will play significant role for film orientation, according to the nature of interaction discussed above. For instance, vdW planes in thermally evaporated Bi_2S_3, Sb_2Se_3, Sb_2S_3, SnS and Bi_2Se_3 films were predominantly oriented parallel to the surface when deposited on inert substrates such as glass or atomically smooth Si[63–67], representing the case in Fig. 6(b). However, on the other substrates with exposed dangling bonds the growth of films with columnar structure comprised of rods (platelets) perpendicular (inclined) to the substrate is expected. High degree of (00*l*) texture with columnar structure of 1D SbSI films was achieved by using anodized TiO_2 nanotubes and Sb_2S_3 as substrates instead of chemically inert Pt[68, 69]. Our experiments indicate that on $MoSe_2$ substrates with basal plane oriented vertically, 1D Sb_2Se_3 tend to grow with (101) and (001) preferred orientation in the wide substrate temperature range presumably because of better lattice matching[70]. Recently, Abdurashid *et al.* systematically investigated the correlation between the growth parameters and the crystallographic orientation of Sb_2Se_3 thin films based on the pulsed laser deposition method[71]. Hence, the growth regime and therefore orientation of low-dimensional material can be controlled by choosing an appropriate substrate or modifying its surface.

The properties of the substrate will dictate the orientation of low-dimensional thin films, however, kinetically limited growth conditions can also be used to steer growth dynamics. During the growth of SnS, increased deposition flux reduced the adatom's surface diffusion length. Consequently instead of thermodynamically favored growth of sparse platelet-like grains, a compact cube-shaped grain morphology was obtained[72]. This also resulted in significant increase in solar cell performance. Under high growth rate conditions, facets with the fastest vertical growth rate will be selectively promoted and eventually dominate film orientation. 1D Sb_2Se_3 thin films deposited under high growth rate regime had explicit orientation of *c*-axis (strong bond) inclined to the surface on various substrates[70]. Inducing kinetically controlled growth conditions can lead to the improved film morphology and desired orientation, especially tuning the growth rate. However to achieve high degree of texture appropriate choice of substrate will be also important.

2.7. Current research status of solar cells based on low-dimensional materials

Many low-dimensional materials have been explored as potential PV absorbers, such as the one-dimensional Bi_2S_3, Sb_2Se_3, Sb_2S_3 and their alloys, two-dimensional $CuSbSe_2$, $CuSbS_2$, GeSe, SnS, and recently Se and BiOI gained an interest for wide bandgap PV application (Table 1). Among them, the record PCE has been achieved in solar cells with $Sb_2(Se,S)_3$ absorber[51]. The symbolic double digit PCE barrier has been broken (10.5%), which has attracted the attention of the worldwide scientific community. This is evident by the significant increase in number of publications including recent review articles regarding Sb-based solar cells[6]. However, the efficiency of the other low-dimensional materials based solar cells except the antimony chalcogenides is generally lower than 5% (Table 1)[7]. This could be related to the lack of dedicated research or intrinsic limitations of specific material (e.g. high anisotropy in carrier mobility). Although visible progress has been made in the last few years, the efficiency is still far behind when compared to the traditional three-dimensional-based solar cells. Most of the solar cells made of low-dimensional materials suffer from high open-circuit voltage (V_{OC}) deficit ($E_g/q - V_{OC}$)[73]. V_{OC} is directly related to the quality of the absorber (presence of deep defects) as

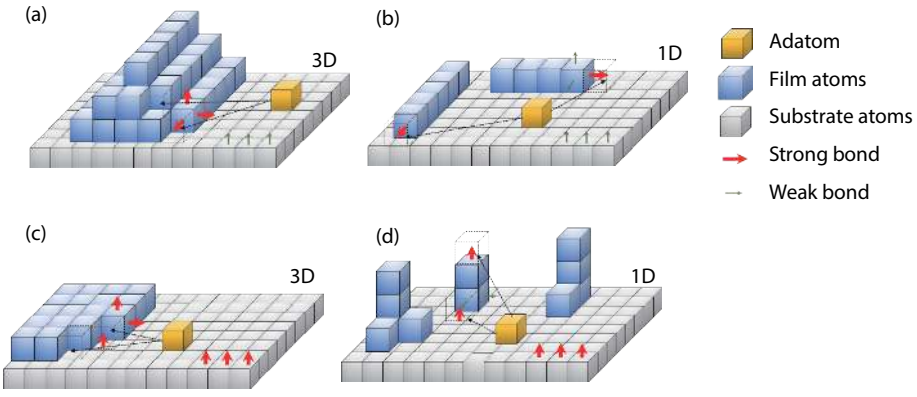

Fig. 6. (Color online) Schematics of growth process of 3D and 1D materials on (a, b) inert and (c, d) strongly interacting substrates. (a) represents an island-like growth mode, whereas (c) layer-by-layer[62].

well as overall device structure (passivation of interfaces). Complex defect chemistry, short carrier lifetime (at the scale of sub-nanoseconds), strong anisotropic conduction band minimum (CBM) and valence band maximum (VBM) found in low-dimensional materials can lead to high V_{OC} deficit. In recent review article on Sb_2Se_3, authors discussed the relationship between V_{OC} deficit and the basic material properties of Sb_2Se_3 (including carrier lifetime, defects, carrier density, and band tail states) and device properties (including recombination mechanism, hole transport layer, and device structure)[73]. Removing, reducing or passivating the deep defects and improving the carrier lifetime are the development trend of solar cell in the future. For instance, a two-stage synthesis by first sputtering high purity Sb layer and subsequently annealing it in reactive Se atmosphere demonstrated a promising route in achieving high V_{OC} (> 0.5 V) Sb_2Se_3 solar cells[74]. Unintentional impurities found in source material can introduce unexpected defects[75]. Depending on the nature of the impurity it can create shallow or deep detrimental defect, therefore it is important to carefully control experimental conditions. In addition, the new fabrication technologies and solar cell designs are also important for the efficiency breakthrough. The use of hydrothermal method and ultrathin absorbers are poised to be the main reasons for the efficiency improvement in record $Sb_2(S,Se)_3$ solar cells[51].

3. Conclusion

We discussed and showed that low-dimensional materials could be applied to device level. This broadens the scope of potential application from nanomaterials to the macroscale devices such as solar cells, photodetectors, light emitting diodes and thermoelectrics. We probed various PV-related material properties and growth mechanism for low-dimensional materials with an aim to provide new insights and design options for functional devices. Low-dimensional materials offer a bright future for various electronic, optic and photonic applications and fabrication of high-quality films with controlled properties will be the next step for their successful implementation.

Acknowledgments

The authors thank the Analytical and Testing Center of HUST and the facility support of the Center for Nanoscale Characterization and Devices (CNCD), WNLO-HUST. This work was supported by the National Natural Science Foundation of China (61725401, 61904058, 61904058), the National Key R&D Program of China (2016YFA0204000), China Postdoctoral Science Foundation Project (2019M662623) and the National Postdoctoral Program for Innovative Talent (BX20190127).

Appendix A. Supplementary materials

Supplementary materials to this article can be found online at https://doi.org/1674-4926/42/3/031701.

References

[1] Philipps S. Photovoltaics report. Fraunhofer Institute for Solar Energy Systems, 2019
[2] Green M A, Hishikawa Y, Dunlop E D, et al. Solar cell efficiency tables (version 52). Pro Photovolt, 2018, 26(7), 427
[3] Alharbi F, Bass J D, Salhi A, et al. Abundant non-toxic materials for thin film solar cells: Alternative to conventional materials. Renew Energ, 2011, 36(10), 2753
[4] Jean J, Brown P R, Jaffe R L, et al. Pathways for solar photovoltaics. Energy Environ Sci, 2015, 8(4), 1200
[5] Lei H, Chen J, Tan Z, et al. Review of recent progress in antimony chalcogenide-based solar cells: Materials and devices. Solar RRL, 2019, 3(6), 1900026
[6] Mavlonov A, Razykov T, Raziq F, et al. A review of Sb_2Se_3 photovoltaic absorber materials and thin-film solar cells. Sol Energy, 2020, 201, 227
[7] Wong L H, Zakutayev A, Major J D, et al. Emerging inorganic solar cell efficiency tables (Version 1). J Phys: Energy, 2019, 1(3), 032001
[8] Yu L, Kokenyesi R S, Keszler D A, et al. Inverse design of high absorption thin-film photovoltaic materials. Adv Energy Mater, 2013, 3(1), 43
[9] Phillips L J, Savory C N, Hutter O S, et al. Current enhancement via a TiO_2 window layer for CSS Sb_2Se_3 solar cells: Performance limits and high V_{OC}. IEEE J Photovolt, 2019, 9(2), 544
[10] Li Z, Liang X, Li G, et al. 9.2%-efficient core-shell structured antimony selenide nanorod array solar cells. Nat Commun, 2019, 10(1), 125
[11] Liu C, Wang L, Tang Y, et al. Vertical single or few-layer MoS_2 nanosheets rooting into TiO_2 nanofibers for highly efficient photocatalytic hydrogen evolution. Appl Catal B, 2015, 164, 1
[12] Chuang H J, Chamlagain B, Koehler M, et al. Low-resistance 2D/2D ohmic contacts: A universal approach to high-performance WSe_2, MoS_2, and $MoSe_2$ transistors. Nano Lett, 2016, 16(3), 1896
[13] Zhao M, Su J, Zhao Y, et al. Sodium-mediated epitaxial growth of

2D ultrathin Sb_2Se_3 flakes for broadband photodetection. Adv Funct Mater, 2020, 30(13), 1909849
[14] Chen Z G, Shi X, Zhao L D, et al. High-performance SnSe thermoelectric materials: Progress and future challenge. Prog Mater Sci, 2018, 97, 283
[15] Wu T, Zhang H. Piezoelectricity in two-dimensional materials. Angew Chem Int Ed, 2015, 54(15), 4432
[16] Niu S, Joe G, Zhao H, et al. Giant optical anisotropy in a quasi-one-dimensional crystal. Nat Photonics, 2018, 12(7), 392
[17] Tian H, Tice J, Fei R, et al. Low-symmetry two-dimensional materials for electronic and photonic applications. Nano Today, 2016, 11(6), 763
[18] Donnay J D H, Harker D. A new law of crystal morphology extending the law of Bravais. Am Mineral, 1937, 22(5), 446
[19] Brandt R E, Poindexter J R, Gorai P, et al. Searching for "defect-tolerant" photovoltaic materials: Combined theoretical and experimental screening. Chem Mater, 2017, 29(11), 4667
[20] Othonos A. Probing ultrafast carrier and phonon dynamics in semiconductors. J App Phys, 1998, 83(4), 1789
[21] Hutter E M, Gélvez-Rueda M C, Osherov A, et al. Direct–indirect character of the bandgap in methylammonium lead iodide perovskite. Nat Mater, 2016, 16, 115
[22] Saliba M, Correa-Baena J P, Wolff C M, et al. How to make over 20% efficient perovskite solar cells in regular (n–i–p) and inverted (p–i–n) architectures. Chem Mater, 2018, 30(13), 4193
[23] Walsh A, Zunger A. Instilling defect tolerance in new compounds. Nat Mater, 2017, 16, 964
[24] Vidal J, Lany S, d'Avezac M, et al. Band-structure, optical properties, and defect physics of the photovoltaic semiconductor SnS. Appl Phys Lett, 2012, 100(3), 032104
[25] Huang Y, Wang C, Chen X, et al. First-principles study on intrinsic defects of SnSe. RSC Advances, 2017, 7(44), 27612
[26] Han D, Du M H, Dai C M, et al. Influence of defects and dopants on the photovoltaic performance of Bi_2S_3: first-principles insights. J Mater Chem A, 2017, 5(13), 6200
[27] Huang M, Xu P, Han D, et al. Complicated and unconventional defect properties of the quasi-one-dimensional photovoltaic semiconductor Sb_2Se_3. ACS Appl Mater Inter, 2019, 11(17), 15564
[28] Qiao J, Kong X, Hu Z X, et al. High-mobility transport anisotropy and linear dichroism in few-layer black phosphorus. Nat Commun, 2014, 5(1), 4475
[29] Zhou Y, Wang L, Chen S, et al. Thin-film Sb_2Se_3 photovoltaics with oriented one-dimensional ribbons and benign grain boundaries. Nat Photonics, 2015, 9(6), 409
[30] Novoselov K S, Mishchenko A, Carvalho A, et al. 2D materials and van der Waals heterostructures. Science, 2016, 353(6298), aac9439
[31] Welch A W, Baranowski L L, Zawadzki P, et al. Accelerated development of $CuSbS_2$ thin film photovoltaic device prototypes. Pro Photovoltaics, 2016, 24(7), 929
[32] Kirchartz T, Rau U. What makes a good solar cell. Adv Energy Mater, 2018, 8(28), 1703385
[33] Gilbert L R, Van Pelt B, Wood C. The thermal activation energy of crystalline Sb_2Se_3. J Phys Chem Solids, 1974, 35(12), 1629
[34] Chen Y, Sun Y, Peng J, et al. Tailoring organic cation of 2D air-Stable organometal halide perovskites for highly efficient planar solar cells. Adv Energy Mater, 2017, 7(18), 1700162
[35] Tsai H, Nie W, Blancon J C, et al. High-efficiency two-dimensional Ruddlesden–Popper perovskite solar cells. Nature, 2016, 536, 312
[36] Nassary M M. Temperature dependence of the electrical conductivity, Hall effect and thermoelectric power of SnS single crystals. J Alloy Compd, 2005, 398(1), 21
[37] Sinsermsuksakul P, Sun L, Lee S W, et al. Overcoming efficiency limitations of SnS-based solar cells. Adv Energy Mater, 2014, 4(15), 1400496
[38] Zhao L D, Tan G, Hao S, et al. Ultrahigh power factor and thermoelectric performance in hole-doped single-crystal SnSe. Science, 2016, 351(6269), 141
[39] Welch A W, Baranowski L L, Peng H, et al. Trade-offs in thin film solar cells with layered chalcostibitephotovoltaic absorbers. Adv Energy Mater, 2017, 7(11), 1601935
[40] Ramasamy K, Sims H, Butler W H, et al. Mono-, few-, and multiple layers of copper antimony sulfide ($CuSbS_2$): A ternary layered sulfide. J Am Chem Soc, 2014, 136(4), 1587
[41] Banu S, Ahn S J, Ahn S K, et al. Fabrication and characterization of cost-efficient $CuSbS_2$ thin film solar cells using hybrid inks. Sol Energ Mat Sol C, 2016, 151, 14
[42] Kautek W. Electronic mobility anisotropy of layered semiconductors: transversal photoconductivity measurements at n-$MoSe_2$. J Phys C, 1982, 15(16), L519
[43] Chen Z, Liu H, Chen X, et al. Wafer-size and single-crystal $MoSe_2$ atomically thin films grown on GaN substrate for light emission and harvesting. ACS Appl Mater Inter, 2016, 8(31), 20267
[44] Evans B, Young P. Optical absorption and dispersion in molybdenum disulphide. Proc R Soc London Ser A, 1965, 284(1398), 402
[45] Wi S, Kim H, Chen M, et al. Enhancement of photovoltaic response in multilayer MoS_2 induced by plasma doping. ACS Nano, 2014, 8(5), 5270
[46] Kyriakos D S, Anagnostopoulos A N. Electrical conductivity of layered GeSe related to extended faults. J App Phys, 1985, 58(10), 3917
[47] Xue D J, Liu S C, Dai C M, et al. GeSe thin-film solar cells fabricated by self-regulated rapid thermal sublimation. J Am Chem Soc, 2017, 139(2), 958
[48] Chakraborty B R, Ray B, Bhattacharya R, et al. Magnetic and electric properties of antimony selenide (Sb_2Se_3) crystals. J Phys Chem Solids, 1980, 41(8), 913
[49] Roy B, Chakraborty B R, Bhattacharya R, et al. Electrical and magnetic properties of antimony sulphide (Sb_2S_3) crystals and the mechanism of carrier transport in it. Solid State Commun, 1978, 25(11), 937
[50] Choi Y C, Lee D U, Noh J H, et al. Highly improved Sb_2S_3 sensitized-inorganic–organic heterojunction solar cells and quantification of traps by deep-level transient spectroscopy. Adv Function Mater, 2014, 24(23), 3587
[51] Wang X, Tang R, Jiang C, et al. Manipulating the electrical properties of $Sb_2(S,Se)_3$ film for high-efficiency solar cell. Adv Energy Mater, 2020, 10, 2002341
[52] Cantarero A, Martinez-Pastor J, Segura A, et al. Transport properties of bismuth sulfide single crystals. Phys Rev B, 1987, 35(18), 9586
[53] Song H, Zhan X, Li D, et al. Rapid thermal evaporation of Bi_2S_3 layer for thin film photovoltaics. Sol Energ Mat Sol C, 2016, 146, 1
[54] Yoshida M, Yamanaka K, Hamakawa Y. Semiconducting and dielectric properties of c-axia oriented SbSI thin film. Jpn J Appl Phys, 1973, 12(11), 1699
[55] Nie R, Yun H S, Paik M J, et al. Efficient solar cells based on light-harvesting antimony sulfoiodide. Adv Energy Mater, 2018, 8(7), 1701901
[56] Hoye R L Z, Lee L C, Kurchin R C, et al. Strongly enhanced photovoltaic performance and defect physics of air-stable bismuth oxyiodide (BiOI). Adv Mater, 2017, 29(36), 1702176
[57] Todorov T K, Singh S, Bishop D M, et al. Ultrathin high band gap solar cells with improved efficiencies from the world's oldest photovoltaic material. Nat Commun, 2017, 8(1), 682
[58] Koma A. New epitaxial growth method for modulated structures using van der Waals interactions. Surf Sci, 1992, 267(1), 29
[59] Yang B, Wang C, Yuan Z, et al. Hydrazine solution processed $CuSbSe_2$: Temperature dependent phase and crystal orientation evolution. Sol Energ Mat Sol C, 2017, 168, 112
[60] Jaccodine R. Surface energy of germanium and silicon. J Electro-

chem Soc, 1963, 110(6), 524
[61] Stevanović V, Hartman K, Jaramillo R, et al. Variations of ionization potential and electron affinity as a function of surface orientation: The case of orthorhombic SnS. Appl Phys Lett, 2014, 104(21), 211603
[62] Venables J A,Spiller G D T. Surface mobilities on solid materials. Boston, MA: Springer, 1983
[63] Rincón M E, Sánchez M, George P J, et al. Comparison of the properties of bismuth sulfide thin films prepared by thermal evaporation and chemical bath deposition. J Solid State Chem, 1998, 136(2), 167
[64] Razykov T M, Shukurov A X, Atabayev O K, et al. Growth and characterization of Sb_2Se_3 thin films for solar cells. Sol Energy, 2018, 173, 225
[65] Mayon Y S, White T P, Wang R, et al. Evaporated and solution deposited planar Sb_2S_3 solar cells: A comparison and its significance. Phys Status Solid A, 2016, 213(1), 108
[66] Nwofe P A, Reddy K T R, Sreedevi G, et al. Single phase, large grain, p-conductivity-type SnS layers produced using the thermal evaporation method. Energy Procedia, 2012, 15, 354
[67] Zhang M, Lv L, Wei Z, et al. Thermal evaporation growth of topological insulator Bi_2Se_3 thin films. Mater Lett, 2014, 123, 87
[68] Solayappan N, Raina K K, Pandey R K, et al. Role of antimony sulfide buffer layers in the growth of ferroelectric antimony sulfo-iodide thin films. J Mater Res, 1997, 12(3), 825
[69] Varghese J, O 'Regan C, Deepak N, et al. Surface roughness assisted growth of vertically oriented ferroelectric SbSI nanorods. Chem Mater, 2012, 24(16), 3279
[70] Kondrotas R, Zhang J, Wang C, et al. Growth mechanism of Sb_2Se_3 thin films for photovoltaic application by vapor transport deposition. Sol Energ Mat Sol C, 2019, 199, 16
[71] Mavlonov A, Shukurov A, Raziq F, et al. Structural and morphological properties of PLD Sb_2Se_3 thin films for use in solar cells. Sol Energy, 2020, 208, 451
[72] Lim D, Suh H, Suryawanshi M, et al. Kinetically controlled growth of phase-pure SnS absorbers for thin film solar cells: Achieving efficiency near 3% with long-term stability using an SnS/CdS heterojunction. Adv Energy Mater, 2018, 8(10), 1702605
[73] Chen C, Tang J. Open-crcuit voltage loss of antimony chalcogenide solar cells: status, origin, and possible solutions. ACS Energy Lett, 2020, 5(7), 2294
[74] Liang G X, Luo Y D, Chen S, et al. Sputtered and selenized Sb_2Se_3 thin-film solar cells with open-circuit voltage exceeding 500 mV. Nano Energy, 2020, 73, 104806
[75] Hobson T D C, Phillips L J, Hutter O S, et al. Isotype heterojunction solar cells using n-type Sb_2Se_3 thin films. Chem Mater, 2020, 32(6), 2621

Rokas Kondrotas earned his Ph.D. in Center for Physical Sciences and Technology (CPST) in 2015. Then he worked as a post-doc in Catalonia Institute for Energy Research for one year and in WNLO for two years. After that, Rokas returned to CPST. His research is thin film solar cells.

Chao Chen received his Ph.D. from Huazhong University of Science and Technology in 2019. Now, he is a postdoctoral fellow at the Wuhan National Laboratory for Optoelectronics, Huazhong University of Science and Technology. His research interests are antimony chalcogenide thin-film solar cells and photodetectors.

Jiang Tang received his Ph.D. from the University of Toronto in 2010. He joined Wuhan National Laboratory for Optoelectronics, Huazhong University of Science and Technology as a full professor in 2012. His research interests include Sb_2Se_3 solar cells, metal halides for X-ray detection, PbS CQD imaging sensor, and halide perovskite LED.